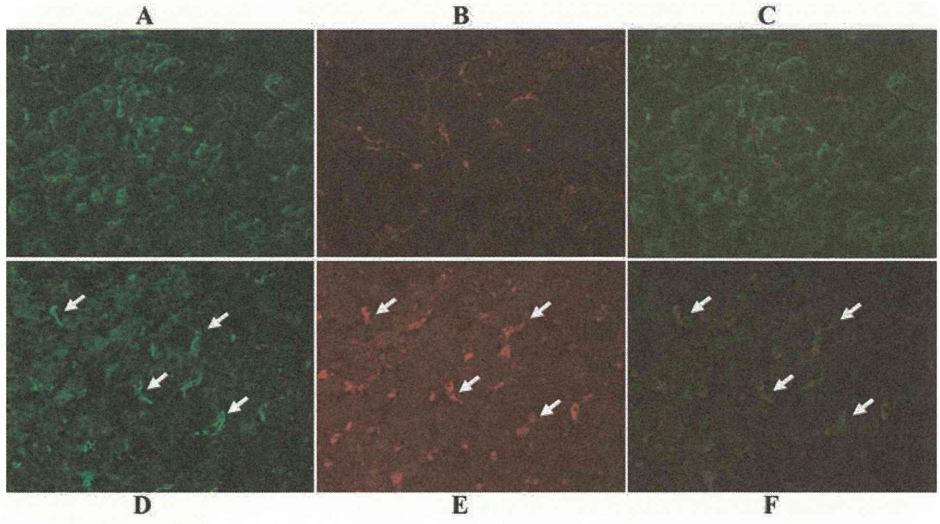

Figure 5 Double immunohistochemistry using chronic viral hepatitis livers. (A, B, C) Monocyte chemoattractant protein-1 receptor (CCR2, green), α-smooth muscle actin (red), and merged image, respectively. Double positive cells indicating CCR2-positive hepatic stellate cells (yellow) are not found. (D, E, F) CCR2 (green), CD68 (red) and merged image, respectively. Double positive cells indicating CCR2-positive Kupffer cells (yellow) are scattered (arrows).

BECs, only the expression of MCP-1 was upregulated, by two proinflammatory cytokines (by IL-1β and, to a lesser degree, by TNF-α) and all TLR ligands in an NF-κB-dependent manner. Because human BECs produced IL-1β when stimulated with TLR ligands,[15] the biliary innate immune response is suggested to be a critical trigger of MCP-1 production.

Bile ductules and their proliferation occur non-specifically in various hepatobiliary diseases. In normal livers, a few bile ductules are recognisable in the portal tract, while in various hepatobiliary diseases, these ductular structures are often increased in number, to be termed 'ductular proliferation' or 'proliferating bile ductules.' Because ductular proliferation was found accompanying interface hepatitis and periductal fibrosis in chronic liver diseases, these biliary elements are thought to take part in disease progression. However, the exact association between ductular proliferation and hepatic fibrogenesis is still unknown. Immunohistochemistry revealed that MCP-1 was expressed in bile ductules in areas of interface hepatitis, whereas normal livers lacked these findings. The ductular reaction predominantly corresponded to interface hepatitis in various chronic hepatobiliary diseases, and these areas were rich in several cytokines caused by immune-mediated (necro)inflammatory reactions against virus-infected hepatocytes and bile-derived PAMPs. Therefore, these microenvironments are suitable for the production of MCP-1 in proliferating bile ductules at the interface.

In damaged liver, HSCs are activated, proliferate and migrate into the injured area in response to the chemoattractive effects of chemokines. MCP-1 is a chemokine attracting monocyte/macrophages and plays a role in persistent inflammation in chronic liver diseases. Marra *et al*[3] reported that MCP-1 attracts HSCs, particularly activated HSCs, to the liver. Innate immunity is known to promote liver fibrosis, and as its mechanism, HSCs are reported to produce MCP-1 via TLR9 signalling.[16] In this study, immunohistochemistry using liver sections from patients with CVH and PBC revealed that αSMA-positive activated HSCs (myofibroblasts) were scattered and accumulated around MCP-1-expressing bile ductules in areas showing interface hepatitis. This finding suggests that MCP-1 derived from BECs plays a role in the chemoattraction of HSCs.

A recent report demonstrated that hepatocytes are also a source of MCP-1 and that hepatocyte-derived MCP-1 induced by a hydrophobic bile acid, taurocholate, chemoattracts HSCs and is associated with the liver fibrosis under cholestatic conditions in cases of paediatric cholestatic liver disease such as biliary atresia. Our immunohistochemical study also confirmed the expression of MCP-1 in periportal hepatocytes, but, in the early stage of CVH and PBC, the MCP-1 derived from bile ductules is speculated to the major effecter, compared with that from hepatocytes, based on the intensity of MCP-1 immunostaining. We also examined the effect of bile acids on the production of MCP-1 in cultured BECs. No bile acids affected the MCP-1 expression in BECs, suggesting that cholestasis could not directly induce the production of MCP-1 in BECs, differing from hepatocytes.

Portal fibroblasts located in portal tracts are fibrogenic cells distinct from HSCs and may be important mediators of biliary fibrosis and cirrhosis. Recently, Kruglov *et al*[17] reported that portal fibroblasts express functional receptors for MCP-1 that are distinct from CCR2 and that the secretion of MCP-1 by BECs induces myofibroblastic transdifferentiation of portal fibroblasts. In fact, the expression of MCP-1 was found in some interlobular bile ducts as well as bile ductules within portal tracts in CVH and PBC (data not shown). This finding suggests that MCP-1-dervied from BECs of these interlobular bile ducts is associated with the migration and activation of portal fibroblasts. However, we speculate that the fibrogenesis associated with portal fibroblasts is mainly associated with the histogenesis of portal sclerosis and expansive fibrous enlargement of portal tracts, not the fibrous extension accompanying interface hepatitis from portal tracts. The close correlation between MCP-1-positive bile ductules and αSMA-positive activated HSCs in the interface area shown in this study supports our contention. Moreover, we examined CHF as a control diseased liver in this study. CHF is different from cirrhosis in which no abnormal biliary channels are seen. In portal tracts of CHF, irregular and newly proliferating bile ducts and ductules rather than congenitally abnormal ductal plates, and cholestasis in these bile ductules are found. However, in parenchyma, the features of chronic cholestasis and interface changes are not prominent. Our previous study reported that the fibrogenesis of CHF is associated with intraportal heparan sulfate proteoglycan and CTGF, but not periportal HSCs.[14] It is true that although proliferating bile ductules were scattered within portal tracts, MCP-1 expression in bile ductules and αSMA-positive HSCs were not found in CHF, suggesting that the MCP-1-mediated migration of HSCs limited in proliferating bile ductules accompanying interface hepatitis of chronic inflammatory hepatobiliary diseases,

Take-home messages

- Biliary epithelial cells express several fibrogenic cytokines (MCP-1, PDGF-B, CTGF, TGF-β1 and endothelin-1), but only MCP-1 expression is upregulated by biliary innate immune reaction and proinflammatory cytokines (IL-1β and TNF-α).
- Proliferating bile ductules in interface areas expressed MCP-1 in diseased livers accompanying αSMA-positive activated hepatic stellate cells.
- MCP-1 derived from biliary epithelial cells plays an important role in the recruitment of hepatic stellate cells to interface areas and the activation of HSCs resulting in the progression of periportal fibrosis.

but not associated with the fibrogenesis in sole cholestatic liver diseases lacking interface changes such as CHF.

Because the receptor of MCP-1, CCR2, is not expressed in human HSCs, HSC migration by MCP-1 occurs independent of CCR2 via an unknown receptor for MCP-1, instead of by CCR2.[3] In fact, double immunohistochemistry in this study revealed that the expression of CCR2 is found not in αSMA-positive HSCs, but in CD68-positive Kupffer cells, suggesting that MCP-1-dervied from BECs could chemoattract Kupffer cells. As mentioned, portal fibroblasts within portal tracts also lack CCR2, but could be attracted by MCP-1 derived from BECs in a CCR2-independent manner.[17] In contrast, Seki *et al*[18] reported that both Kupffer cells and HSCs express CCR2 in mice but that these differences might be explained by differences between humans and mice.

Various types of inflammation including infection-triggered inflammation are causative factors to induce hepatic fibrosis in chronic liver diseases. Particularly, HSCs are critical for hepatic fibrogenesis, and MCP-1 is an important cytokine associated with HSC migration in fibrogenic areas. Therefore, the identification of MCP-1-producing cells and the clarification of the mechanism of MCP-1 production are mandatory to help regulate hepatic fibrosis and treat liver fibrosis. This study revealed that BECs are a source of MCP-1 in some hepatobiliary diseases, and the production of MCP-1 is induced by inflammatory cytokines and biliary innate immune responses. Proliferating bile ductules are thought to be part of a non-specific reaction in various hepatobiliary diseases, but this study suggests that they are closely associated with the progression of periportal fibrosis via MCP-1 derived from biliary innate immunity. Because MCP-1 is thought to be a key mediator of hepatic fibrosis, it is a potential therapeutic target in inflammatory hepatobiliary diseases with hepatic fibrosis.

Funding This work was supported by Grants-in-aid for Scientific Research from the Ministry of Health, Labour and Welfare of Japan and Grants-in-Aid for Scientific Research (C) from the Ministry of Education, Culture, Sports, Science and Technology of Japan.

Competing interests None.

Patient consent Obtained.

Ethics approval This study was approved by the Kanazawa University Ethics Committee.

Contributors KH and YN conceived and carried out the experiments; AO, MH, YS, SI, XSR, HI, HO, SK and AK conceived the experiments and analysed data; MC carried out the experiments. All authors were involved in writing the paper and had final approval of the submitted and published versions.

Provenance and peer review Not commissioned; externally peer reviewed.

REFERENCES

1. **Friedman SL,** Arthur MJ. Activation of cultured rat hepatic lipocytes by Kupffer cell conditioned medium. Direct enhancement of matrix synthesis and stimulation of cell proliferation via induction of platelet-derived growth factor receptors. *J Clin Invest* 1989;**84**:1780–5.
2. **Friedman SL,** Yamasaki G, Wong L. Modulation of transforming growth factor beta receptors of rat lipocytes during the hepatic wound healing response. Enhanced binding and reduced gene expression accompany cellular activation in culture and in vivo. *J Biol Chem* 1994;**269**:10551–8.
3. **Marra F,** Romanelli RG, Giannini C, *et al*. Monocyte chemotactic protein-1 as a chemoattractant for human hepatic stellate cells. *Hepatology* 1999;**29**:140–8.
4. **Ramm GA,** Shepherd RW, Hoskins AC, *et al*. Fibrogenesis in pediatric cholestatic liver disease: role of taurocholate and hepatocyte-derived monocyte chemotaxis protein-1 in hepatic stellate cell recruitment. *Hepatology* 2009;**49**:533–44.
5. **Kinnman N,** Housset C. Peribiliary myofibroblasts in biliary type liver fibrosis. *Front Biosci* 2002;**7**:d496–503.
6. **Harada K,** Isse K, Nakanuma Y. Interferon gamma accelerates NF-kappaB activation of biliary epithelial cells induced by Toll-like receptor and ligand interaction. *J Clin Pathol* 2006;**59**:184–90.
7. **Harada K,** Ohba K, Ozaki S, *et al*. Peptide antibiotic human beta-defensin-1 and -2 contribute to antimicrobial defense of the intrahepatic biliary tree. *Hepatology* 2004;**40**:925–32.
8. **Harada K,** Ohira S, Isse K, *et al*. Lipopolysaccharide activates nuclear factor-kappaB through Toll-like receptors and related molecules in cultured biliary epithelial cells. *Lab Invest* 2003;**83**:1657–67.
9. **Harada K,** Sato Y, Itatsu K, *et al*. Innate immune response to double-stranded RNA in biliary epithelial cells is associated with the pathogenesis of biliary atresia. *Hepatology* 2007;**46**:1146–54.
10. **Nakanuma Y,** Hoso M, Sanzen T, *et al*. Microstructure and development of the normal and pathologic biliary tract in humans, including blood supply. *Microsc Res Tech* 1997;**38**:552–70.
11. **Isse K,** Harada K, Nakanuma Y. IL-8 expression by biliary epithelial cells is associated with neutrophilic infiltration and reactive bile ductules. *Liver Int* 2007;**27**:672–80.
12. **Harada K,** Kono N, Tsuneyama K, *et al*. Cell-kinetic study of proliferating bile ductules in various hepatobiliary diseases. *Liver* 1998;**18**:277–84.
13. **Nakanuma Y,** Zen Y, Harada K, *et al*. Application of a new histological staging and grading system for primary biliary cirrhosis to liver biopsy specimens: Interobserver agreement. *Pathol Int* 2010;**60**:167–74.
14. **Ozaki S,** Sato Y, Yasoshima M, *et al*. Diffuse expression of heparan sulfate proteoglycan and connective tissue growth factor in fibrous septa with many mast cells relate to unresolving hepatic fibrosis of congenital hepatic fibrosis. *Liver Int* 2005;**25**:817–28.
15. **Harada K,** Shimoda S, Sato Y, *et al*. Periductal interleukin-17 production in association with biliary innate immunity contributes to the pathogenesis of cholangiopathy in primary biliary cirrhosis. *Clin Exp Immunol* 2009;**157**:261–70.
16. **Gabele E,** Muhlbauer M, Dorn C, *et al*. Role of TLR9 in hepatic stellate cells and experimental liver fibrosis. *Biochem Biophys Res Commun* 2008;**376**:271–6.
17. **Kruglov EA,** Nathanson RA, Nguyen T, *et al*. Secretion of MCP-1/CCL2 by bile duct epithelia induces myofibroblastic transdifferentiation of portal fibroblasts. *Am J Physiol Gastrointest Liver Physiol* 2006;**290**:G765–71.
18. **Seki E,** de Minicis S, Inokuchi S, *et al*. CCR2 promotes hepatic fibrosis in mice. *Hepatology* 2009;**50**:185–97.

Monocyte chemoattractant protein-1 derived from biliary innate immunity contributes to hepatic fibrogenesis

Kenichi Harada, Mayumi Chiba, Atsushi Okamura, et al.

J Clin Pathol 2011 64: 660-665 originally published online April 27, 2011
doi: 10.1136/jclinpath-2011-200040

OPEN ACCESS Freely available online

PLOS ONE

Tumor Necrosis Factor-α Promotes Cholestasis-Induced Liver Fibrosis in the Mouse through Tissue Inhibitor of Metalloproteinase-1 Production in Hepatic Stellate Cells

Yosuke Osawa[1,2]*, Masato Hoshi[3], Ichiro Yasuda[2], Toshiji Saibara[4], Hisataka Moriwaki[2], Osamu Kozawa[1]

1 Department of Pharmacology, Gifu University Graduate School of Medicine, Gifu, Gifu, Japan, **2** Department of Gastroenterology, Gifu University Graduate School of Medicine, Gifu, Gifu, Japan, **3** Faculty of Health Science, Suzuka University of Medical Science, Suzuka, Mie, Japan, **4** Department of Gastroenterology and Hepatology, Kochi University School of Medicine, Nankoku, Kochi, Japan

Abstract

Tumor necrosis factor (TNF)-α, which is a mediator of hepatotoxicity, has been implicated in liver fibrosis. However, the roles of TNF-α on hepatic stellate cell (HSC) activation and liver fibrosis are complicated and remain controversial. To explore this issue, the role of TNF-α in cholestasis-induced liver fibrosis was examined by comparing between TNF-$\alpha^{-/-}$ mice and TNF-$\alpha^{+/+}$ mice after bile duct ligation (BDL). Serum TNF-α levels in mice were increased by common BDL combined with cystic duct ligation (CBDL+CDL). TNF-α deficiency reduced liver fibrosis without affecting liver injury, inflammatory cell infiltration, and liver regeneration after CBDL+CDL. Increased expression levels of collagen α1(I) mRNA, transforming growth factor (TGF)-β mRNA, and α-smooth muscle actin (αSMA) protein by CBDL+CDL in the livers of TNF-$\alpha^{-/-}$ mice were comparable to those in TNF-$\alpha^{+/+}$ mice. Exogenous administration of TNF-α decreased collagen α1(I) mRNA expression in isolated rat HSCs. These results suggest that the reduced fibrosis in TNF-$\alpha^{-/-}$ mice is regulated in post-transcriptional level. Tissue inhibitor of metalloproteinase (TIMP)-1 plays a crucial role in the pathogenesis of liver fibrosis. TIMP-1 expression in HSCs in the liver was increased by CBDL+CDL, and the induction was lower in TNF-$\alpha^{-/-}$ mice than in TNF-$\alpha^{+/+}$ mice. Fibrosis in the lobe of TIMP-$1^{-/-}$ mice with partial BDL was also reduced. These findings indicate that TNF-α produced by cholestasis can promote liver fibrosis via TIMP-1 production from HSCs. Thus, targeting TNF-α and TIMP-1 may become a new therapeutic strategy for treating liver fibrosis in cholestatic liver injury.

Citation: Osawa Y, Hoshi M, Yasuda I, Saibara T, Moriwaki H, et al. (2013) Tumor Necrosis Factor-α Promotes Cholestasis-Induced Liver Fibrosis in the Mouse through Tissue Inhibitor of Metalloproteinase-1 Production in Hepatic Stellate Cells. PLoS ONE 8(6): e65251. doi:10.1371/journal.pone.0065251

Editor: Simon Afford, University of Birmingham, United Kingdom

Received January 14, 2013; **Accepted** April 23, 2013; **Published** June 3, 2013

Funding: This work was supported by grants from the Takeda Science Foundation, the Kondou Kinen Medical Foundation, the Kurozumi Medical Foundation, the Yasuda Medical Foundation, the Senshin Medical Research Foundation, and by a Grant-in-Aid for Scientific Research from the Ministry of Education, Science, Sports, and Culture of Japan (23790787). The funders had no role in study design, data collection and analysis, decision to publish, or preparation of the manuscript.

Competing Interests: The authors have declared that no competing interests exist.

* E-mail: osawa-gif@umin.ac.jp

Introduction

Chronic liver injury is characterized by hepatocyte cell death, hepatic inflammation, and activation of hepatic stellate cell (HSC), a major fibrogenic cell type in the liver [1]. Advanced liver fibrosis disrupts the normal architecture of the liver, causing hepatocellular dysfunction and portal hypertension. Cholestasis is associated with many liver diseases, and bile duct ligation (BDL) has been used in an animal model of chronic liver injury because it duplicates the hepatocyte damage, HSC activation, and liver fibrosis observed in human liver diseases. In the BDL model, accumulation of bile acids by biliary obstruction is thought to contribute to the liver damage [2,3]. Bile acids are amphipathic molecules synthesized by hepatocytes and have detergent action required for lipid absorption. Exposure of hepatocytes to elevated concentrations of bile acid results in cell death [3,4], and bile acid-associated death receptor-mediated cell death is one of the common mechanism for cholestatic hepatocyte injury [5]. Tumor necrosis factor (TNF)-α, which is the mediator of hepatotoxicity in many liver diseases [6], is elevated by common BDL (CBDL) [7], and the liver injury and fibrosis induced by CBDL are reduced in TNF-$\alpha^{-/-}$ mice [8] and TNF receptor (TNFR)$1^{-/-}$ mice [9]. In addition, liver fibrosis induced by carbon tetrachloride (CCl_4) is also reduced in TNFR$1^{-/-}$ mice [10]. Thus, TNF-α has been thought to be crucial for liver injury and subsequent liver fibrosis. However, TNF-α alone does not induce hepatocyte cell death, and the sensitization of hepatocytes by D-galactosamine (GalN) is required for TNF-α-induced liver injury in mice [11,12]. In contrast to its negative regulatory effects, TNF-α has a protective role in liver injury [13] and is required for liver regeneration [14]. Furthermore, TNF-α inhibits collagen α1(I) mRNA expression in HSCs [15,16,17]. Thus, the roles of TNF-α on HSCs activation and liver fibrosis are complicated and remain controversial.

Progression of liver fibrosis is associated with the inhibition of matrix degradation [18]. Matrix degradation is induced by the matrix metalloproteinase (MMP) family of enzymes; MMP-2, -3, and -9 are associated with the liver. Tissue inhibitor of metalloproteinase (TIMP)-1, the most important endogenous inhibitor of most MMPs, plays a crucial role in the pathogenesis of liver fibrosis, and its expression in HSCs is enhanced by TNF-α [9,19,20]. In human liver fibrosis, TIMP-1 expression is increased compared to that in the normal liver [18]. Overexpression of

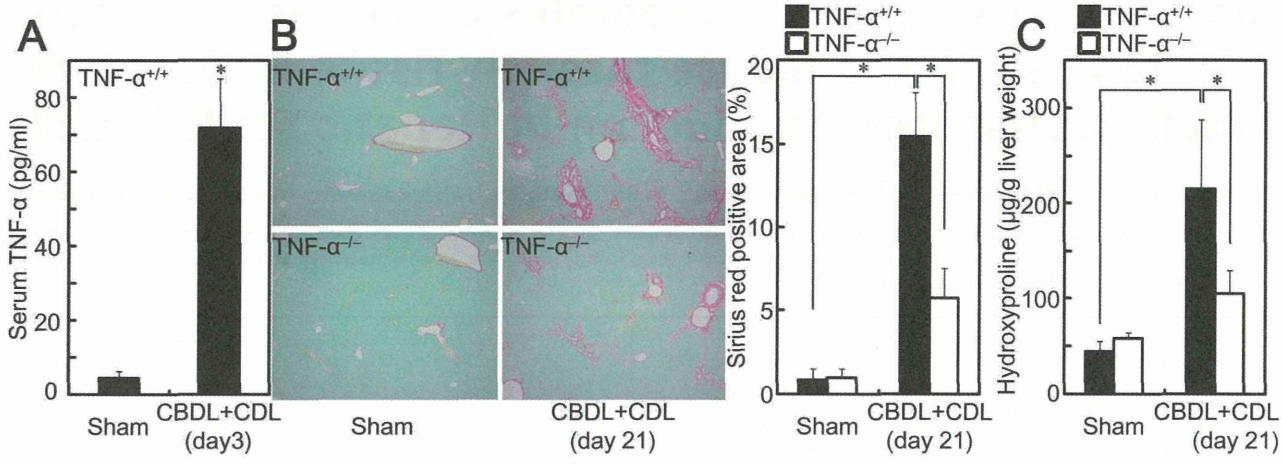

Figure 1. TNF-α deficiency reduced liver fibrosis after CBDL+CDL. TNF-$\alpha^{+/+}$ and TNF-$\alpha^{-/-}$ mice received CBDL+CDL. The animals were sacrificed on 3 (A) or 21 (B, C) days after the surgery. (A) Serum TNF-α levels were measured by ELISA. (B, C) Collagen deposition was assessed by Sirius red staining (B, original magnification: 40×, graph in right panel) and measurement of hydroxyproline content (C). Data are mean ± SD from at least 5 independent experiments. *, $P<0.05$ using a 2-tailed Student's t-test.
doi:10.1371/journal.pone.0065251.g001

MMP-9 in the mouse liver, using an adenovirus vector, reduces liver fibrosis after CCl_4 treatment [21]. Moreover, antagonization of TIMP-1 by a catalytically inactive mutant MMP-9 [21] or by TIMP-1 neutralizing antibody [22] decreases liver fibrosis. Inversely, transgenic mice overexpressing TIMP-1 in the liver show increased liver fibrosis after CCl_4 treatment, whereas TIMP-1 overexpression alone does not result in liver fibrosis [23]. In addition to its role in inhibiting matrix degradation, TIMP-1 promotes survival and proliferation of liver cells. TIMP-$1^{-/-}$ mice demonstrate impaired liver injury and hepatocyte proliferation after hepatic ischemia and reperfusion [24] and demonstrate exacerbated liver injury and fibrosis induced by CCl_4 [25]. Thus, the effects of TIMP-1 on liver injury and fibrosis depend on pathophysiological condition, and its role on fibrosis after cholestatic liver injury remains unclear. To attempt to clarify the precise roles, this study investigated the involvement of TNF-α and TIMP-1 in the progression of fibrosis after cholestatic liver injury.

Materials and Methods

Ethics Statement

The experiments were conducted in accordance with the institutional guidelines and the protocol was approved by the Animal Research Committee of Gifu University (Permit Numbers: 23-3 and 23-38). All surgery was performed under anesthesia, and all efforts were made to minimize suffering.

Animals

Wister male rats and male wild-type mice (C57Bl/6J), TNF-α-deficient mice (TNF-$\alpha^{-/-}$), and TIMP-1-deficient mice (TIMP-$1^{-/-}$) were used for this study. TNF-$\alpha^{-/-}$ mice (#5540, C57Bl/6 background) and TIMP-$1^{-/-}$ mice (#6243, C57Bl/6 background) were obtained from Jackson Laboratory (Bar Harbor, ME, USA), and wild-type C57Bl/6J mice and Wister male rats were from Japan SLC (Shizuoka, Japan).

Bile Duct Ligation (BDL)

Eight-10 week-old male mice were used for studies. To perform common BDL and cystic duct ligation (CBDL+CDL), the peritoneal cavity was opened under anesthesia and the common bile duct was double ligated below the bifurcation, single ligated above the pancreas, and cut between the ligatures. In addition, the cystic duct was single ligated. The left hepatic duct was single ligated for partial BDL (PBDL) as previously reported [26,27]. As necessary, GalN (Nacalai Tesque, Kyoto, Japan) (20 mg/mouse) was intraperitoneally administrated at 30 min before the surgery. On days 1, 3, 7, 21 after the surgery, mice were humanely killed.

Measurement of Serum TNF-α

Mouse serum TNF-α level was measured by ELISA (Thermo Scientific, Rockford, IL, USA).

Histological Analysis

The liver was fixed with 10% formalin, sectioned, and stained with H&E. Collagen deposition was stained with Sirius red (saturated picric acid containing 0.1% DirectRed 80 and 0.1% FastGreen FCF). The Sirius red positive area was quantitated using the ImageJ software (U.S. National Institutes of Health; http://rsb.info.nih.gov/ij/) and shown as a percentage of the total section area. Apoptosis was assessed by the terminal deoxynucleotidyl transferase-dUTP nick end labeling (TUNEL) assay (Promega, Madison, WI, USA, #G7132). The number of TUNEL positive nuclei was determined in 10 randomly selected fields. F4/80, CD3, Ki67, TIMP-1, and desmin were stained with anti-F4/80 (Santa Cruz Biotechnology, Santa Cruz, CA, USA, sc-52664), CD3 (Abcam, Cambridge, MA, USA, ab16669), Ki67 (Thermo scientific, RM-9106), TIMP-1 (R&D Systems, Minneapolis, MN, USA), desmin (Lab Vision, Fremont, CA, USA) antibodies using the Vectastain Elite ABC Kit (Vector Laboratories, Burlingame, CA, USA). Diaminobenzidine tetrahydrochloride was used as peroxidase substrate and sections were counterstained with hematoxylin. The immunostained-positive area of F4/80 was determined using ImageJ software and shown as a percentage of the total section area. The number of CD3 or Ki67-expressing cells was determined in 10 randomly selected fields. In some experiments, fluorescent-dye labeled secondary antibodies (Alexa Fluor 488 anti-rabbit for desmin and Alexa Fluor 594 anti-goat for TIMP-1) (Invitrogen, Carlsbad, CA, USA) were used for detection of primary antibodies as previously reported [28].

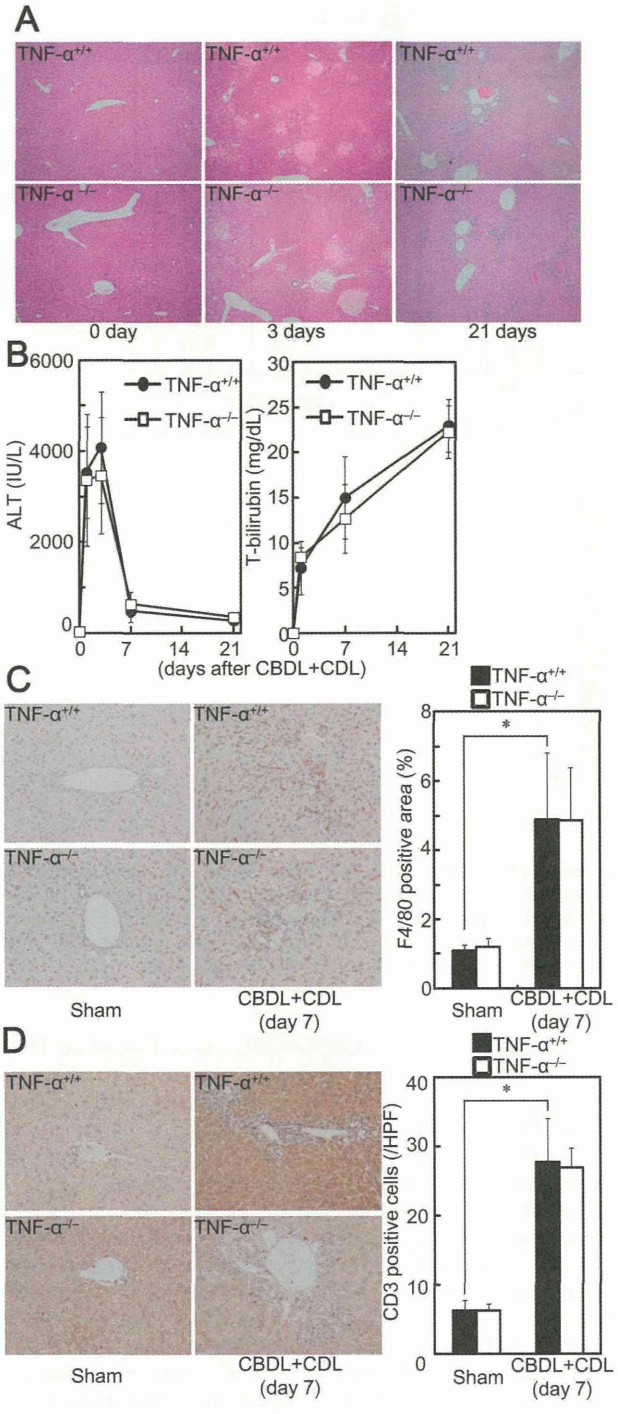

Figure 2. TNF-α deficiency did not affect CBDL+CDL-induced liver injury. TNF-$\alpha^{+/+}$ and TNF-$\alpha^{-/-}$ mice received CBDL+CDL. The animals were sacrificed at the indicated times. (A) The injured lesion in the livers was assessed by H&E staining (original magnification: 40×). (B) Serum ALT and total bilirubin levels were compared at the indicated times. (C) Expression of F4/80 in the livers was examined by immunohistochemistry (original magnification: 200×). F4/80 positive area was compared (right panel). (D) $CD3^+$ cells in the livers were examined by immunohistochemistry (original magnification: 200×). Number of $CD3^+$ cells was compared. Data are mean ± SD from at least 5 independent experiments. *, $P<0.05$ vs. sham using a 2-tailed Student's t-test.

doi:10.1371/journal.pone.0065251.g002

Hydroxyproline Measurement

Hydroxyproline was measured for assessment of collagen content. The extracted liver protein was hydrolyzed in 6 M HCl (100°C, 24 h). The samples were neutralized with LiOH, and hydroxyproline was measured using a high-performance liquid chromatographic analyzer (Jasco, Hitachi, and Shimazu, Japan).

Isolation of Rat Primary HSC

Rat primary HSCs were isolated as previously described [29]. The liver was perfused via the portal vein with collagenase (Wako, Osaka, Japan) and pronase E (EMD Chemicals, Gibbstown, NJ, USA). After digestion, the cell suspension was filtered through nylon mesh and purified via 8.2% Nycodenz (Axis-Shield, Oslo, Norway) gradient centrifugation. The isolated HSCs were cultured in uncoated plastic dishes with DMEM (Sigma-Aldrich, St. Louis, MO, USA) supplemented with 10% fetal bovine serum and antibiotic solution at 37°C in 5% CO_2. After plating for 4 h, the medium was changed to DMEM with 10% fetal bovine serum and antibiotics containing TNF-α (30 ng/ml, R&D Systems) for 72 h. The purity of HSCs was always 95% as determined by their typical starlike shape and abundant lipid droplets with vitamin A autofluorescence.

Western Blot

Electrophoresis of protein extracts and blotting were performed with anti-cyclin E (Santa Cruz Biotechnology, sc-481), glyceraldehyde-3-phosphate dehydrogenase (GAPDH) (Cell Signaling Technology, Danvers, MA, USA, #2118), α-smooth muscle actin (αSMA) (Sigma-Aldrich, A2547), and TIMP-1 antibodies. Then, the membrane was incubated with the horseradish peroxidase-coupled secondary antibodies (Santa Cruz Biotechnology). Detection was performed with an ECL system (Amersham Biosciences, Buckinghamshire, UK), and the protein bands were quantified by densitometry using the ImageJ software.

Quantitative Real Time RT-PCR

RNA was extracted from liver tissue and cultured cells using the RNeasy and DNase Kits (Qiagen, Valencia, CA, USA) and was reverse-transcribed using the High-Capacity cDNA Reverse Transcription Kit (Applied Biosystems, Foster City, CA, USA). Quantitative real-time RT-PCR was performed using the SYBR Premix Ex Taq (Takara, Shiga, JAPAN) for mouse and rat TIMP-1 (forward; TGGGGAACCCATGAATTTAG, reverse; TCTGGCATCCTCTTGTTGC), rat collagen type I α1 (forward; TAGGCCATTGTGTATGCAGC, reverse; ACATGTTCAGCTTTGTGGACC), mouse αSMA (forward; GTTCAGTGGTGCCTCTGTCA, reverse; ACTGGGACGACATGGAAAAG), rat αSMA (forward; GTTCAGCGGCGCCTCCGTTA, reverse; ACTGGGACGACATGGAAAAG), rat and mouse desmin (forward; CTCGGAAGTTGAGAGCAGAGA, reverse; GTGAAGATGGCCTTGGATGT), mouse vimentin (forward; ACCGCTTTGCCAACTACAT, reverse; TTGTCCCGCTCCACCTC), and rat chemokine (C-C motif) ligand 5 (CCL5) (forward; CCACTTCTTCTCTGGGTTGG, reverse; GTGCCCACGTGAAGGAGTAT), and probe-primers sets (Applied Biosystems) for mouse procollagen type I α1 (Mm00801666g1), mouse transforming growth factor (TGF)-β1 (Mm00441724m1) and 18S ribosomal RNA (Hs99999901s1) with the LightCycler 480 (Roche Applied Science, Mannheim, Germany). The changes were normalized based on 18S rRNA values.

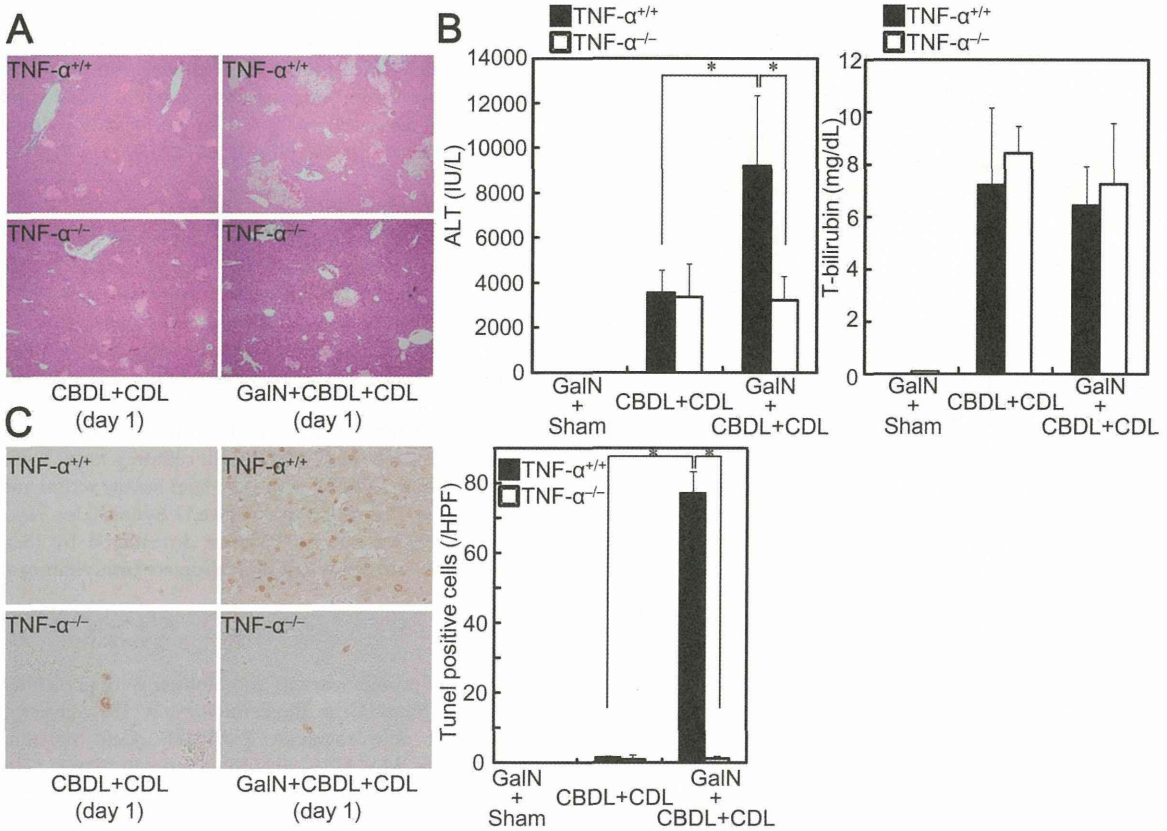

Figure 3. TNF-α-mediated increase of liver injury and hepatocyte apoptosis after CBDL+CDL was induced only in GalN sensitized mice. TNF-$\alpha^{+/+}$ and TNF-$\alpha^{-/-}$ mice were treated with or without GalN (20 mg) and subjected to CBDL+CDL. The animals were sacrificed 24 h after the surgery. (A) The injured lesions in the livers were assessed by H&E staining (original magnification: 40×). (B) Serum ALT and total bilirubin levels were compared. (C) Apoptotic nuclei were identified by TUNEL staining (original magnification: 400×). Numbers of TUNEL-positive cells were compared (right panel). Data are mean ± SD from at least 5 independent experiments. *, $P<0.05$ using a 2-tailed Student's t-test.
doi:10.1371/journal.pone.0065251.g003

Gelatin Zymography

Gelatin zymography was performed with extracted proteins from the liver (50 μg) as described previously [30]. Frozen livers were homogenized in lysis buffer (20 mmol/L HEPES [pH 7.5], 150 mmol/L NaCl, 10 mmol/L CHAPS) and the homogenates were centrifuged at 20,000*g* for 20 min at 4°C. Proteins from supernatant were separated in 7.5% polyacrylamide gel containing 1 mg/mL of gelatin. The gels were equilibrated in developing buffer (50 mmol/L Tris [pH 7.4], 200 mmol/L NaCl, 10 mmol/L CaCl2, 0.02% sodium azaid). The gel was stained with 0.5% Coomassie Blue R-250, followed by destaining. Gelatinolytic activity was detected as clear bands on a dark blue background.

Statistical Analysis

Data are expressed as the mean ± SD of data collected from at least 5 independent experiments. Data between groups were analyzed by the 2-tailed Student's *t*-test. A *P* value of less than 0.05 was an indication of statistical significance.

Results

Deficiency of TNF-α Reduces CBDL+CDL-induced Liver Fibrosis

Serum TNF-α level was increased by CBDL+CDL in wild-type mice (Figure 1A), as previously reported [7]. To explore the roles of TNF-α on liver fibrosis, CBDL+CDL was performed on TNF-$\alpha^{-/-}$ mice. Fibrosis was induced in CBDL+CDL mice, as demonstrated by Sirius red staining and hydroxyproline content (Figure 1B, C). CBDL +CDL livers of TNF-$\alpha^{-/-}$ mice showed reduced fibrosis, compared to those of TNF-$\alpha^{+/+}$ mice (Figure 1B, C), suggesting that TNF-α contributes to liver fibrosis.

Liver fibrosis is induced by liver cell damage and inflammatory cell infiltration with impaired hepatocyte regeneration. However, TNF-$\alpha^{-/-}$ mice showed liver injury (Figure 2A), increased serum alanine aminotransferase (ALT) and total bilirubin (Figure 2B), infiltrated F4/80^{+} macrophages (Figure 2C), and number of infiltrated CD3^{+} lymphocytes (Figure 2D) after CBDL +CDL to a similar degree as was observed for TNF-$\alpha^{+/+}$ mice, suggesting that TNF-α is not related to liver injury and inflammatory cell infiltration in CBDL+CDL mice. To confirm the irrelevance of TNF-α to liver injury, the mice were pretreated with GalN, which increases sensitivity to TNF-α-induced liver damage and hepatocyte apoptosis [31], and subsequently received CBDL+CDL. GalN treatment alone did not induce liver injury or fibrosis (data not shown). Liver injury by CBDL+CDL was exacerbated in the GalN-pretreated mice (Figure 3A). Serum ALT levels were also higher in the GalN-pretreated mice than in the non-treated mice, although total bilirubin was comparable (Figure 3B), suggesting that hepatocyte cell death was exacerbated in the GalN-pretreated mice without increased cholestasis. Moreover, TUNEL-positive hepatocytes were increased in GalN-treated mice that received

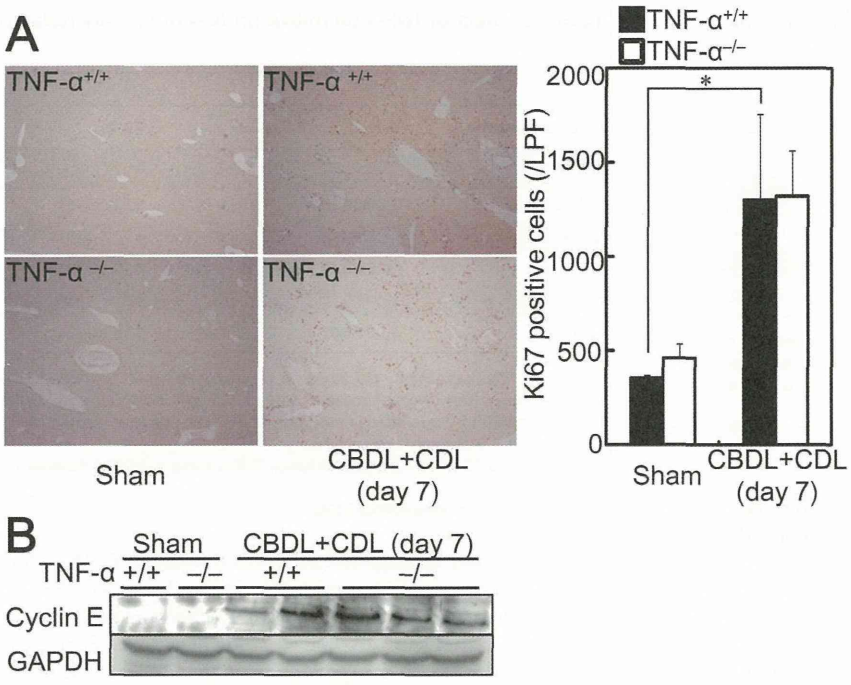

Figure 4. TNF-α deficiency did not affect hepatocyte regeneration after CBDL+CDL. TNF-$\alpha^{+/+}$ and TNF-$\alpha^{-/-}$ mice received CBDL+CDL. The animals were sacrificed 7 days after the surgery. (A) Expression of Ki67 in the livers was examined by immunohistochemistry (original magnification: 40×). Number of $Ki67^{+}$ cells was compared (right panel). Data are mean ± SD from at least 5 independent experiments. *, $P<0.05$ using a 2-tailed Student's t-test. (B) The protein extracts from the livers were subjected to SDS-PAGE and immunoblotting was performed with anti-cyclin E and -GAPDH antibodies. The results shown are representative of at least 3 independent experiments.
doi:10.1371/journal.pone.0065251.g004

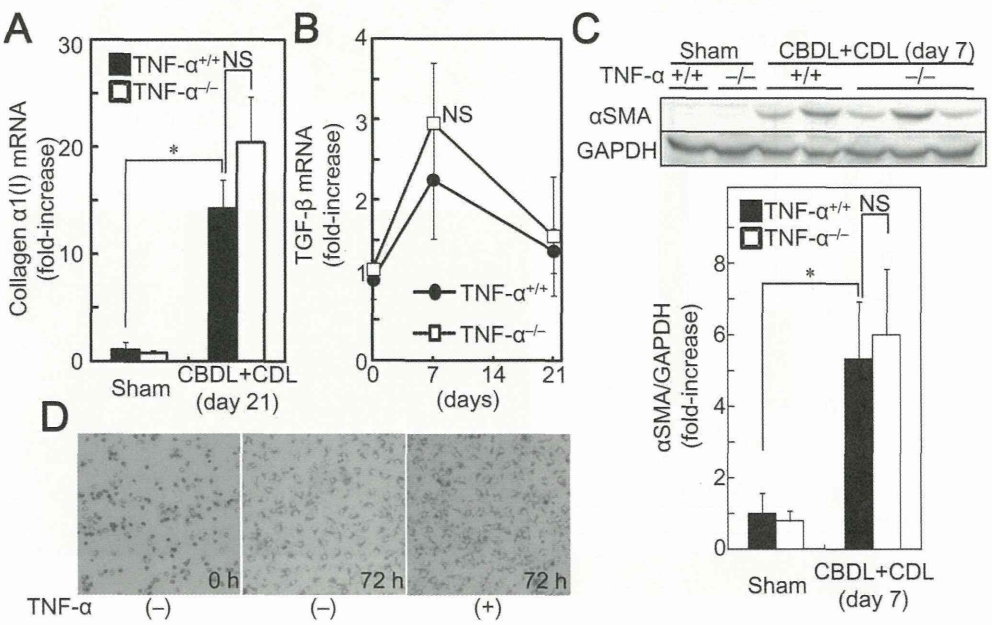

Figure 5. TNF-α deficiency did not affect collagen α1(I) mRNA expression and HSC activation in the livers of mice after CBDL+CDL. TNF-$\alpha^{+/+}$ and TNF-$\alpha^{-/-}$ mice received CBDL+CDL. The animals were sacrificed at the indicated times. (A, B) mRNA levels of collagen α1(I) (A) and TGF-β1 (TGF-β) (B) in the livers were determined by quantitative real time RT-PCR. (C) The protein extracts from the livers were analyzed by SDS-PAGE, and immunoblotting was performed with anti-αSMA and -GAPDH antibodies. The results shown are representative of at least 5 independent experiments. Relative densitometric intensity of αSMA was determined for each protein band and normalized to GAPDH (bottom panels). (D) Primary rat HSCs were incubated on plastic dishes for 72 h with or without 30 ng/mL TNF-α. Bright field images of the HSCs are shown. Data are mean ± SD from at least 5 independent experiments. *, $P<0.05$ using a 2-tailed Student's t-test. NS, not significant.
doi:10.1371/journal.pone.0065251.g005

Table 1. Changes in the mRNA profiles of the liver after CBDL+CDL in TNF-$\alpha^{-/-}$ mice TNF-$\alpha^{+/+}$ and TNF-$\alpha^{-/-}$ mice received CBDL+CDL.

	sham		CBDL+CDL	
	TNF-$\alpha^{+/+}$	TNF-$\alpha^{-/-}$	TNF-$\alpha^{+/+}$	TNF-$\alpha^{-/-}$
αSMA	1.00±0.64	1.36±0.25	5.43±0.98*	6.32±1.22
desmin	1.00±0.36	1.19±0.17	1.73±0.28*	1.76±0.69
vimentin	1.00±0.18	1.22±0.23	2.77±0.82*	3.66±0.77

The animals were sacrificed 7 days after the surgery. mRNA levels of αSMA, desmin, and vimentin in the livers were determined by quantitative real time RT-PCR. Results are presented as means ± SD of data collected from at least 5 independent experiments.
*P<0.05 versus sham-operated TNF-$\alpha^{+/+}$ mice using a 2-tailed Student's t-test.
doi:10.1371/journal.pone.0065251.t001

Table 2. Effect of TNF-α on mRNA profiles of primary isolated rat HSCs.

Incubation time	0 h	72 h	72 h
TNF-α	(–)	(–)	(+)
collagen α1(I)	1.00±0.12	7.95±0.85	3.52±0.45*
αSMA	1.00±0.16	7.44±0.69	6.71±0.78
desmin	1.00±0.17	2.20±0.11	4.32±0.44*
CCL5	1.00±0.23	0.15±0.02	1.63±0.25*
TIMP-1	1.00±0.07	2.25±0.22	3.76±0.33*

Primary rat HSCs were incubated on plastic dishes for 72 h with or without TNF-α (30 ng/mL). mRNA levels of collagen α1(I), αSMA, desmin, CCL5, and TIMP-1 were determined by quantitative real time RT-PCR (E). Data are mean ± SD from at least 6 independent experiments.
*P<0.05 versus 72 h cultured HSCs without TNF-α using a 2-tailed Student's t-test.
doi:10.1371/journal.pone.0065251.t002

CBDL+CDL (Figure 3C). These effects of GalN were blunted in TNF-$\alpha^{-/-}$ mice (Figure 3). TNF-α treatment alone does not induce hepatocyte cell death, and the sensitization of hepatocytes by GalN is required for TNF-α-induced liver injury in mice [11,12]. These previous findings, in conjunction with our results, suggest that the liver damage increments caused by GalN combination is induced by the TNF-α produced by CBDL+CDL; TNF-α causes liver damage only when the hepatocytes are sensitized by GalN in CBDL+CDL mice, and TNF-α does not contribute to liver damage in CBDL+CDL without GalN. Thus, this liver damage may be primarily induced by accumulated cytotoxic bile acids. Furthermore, CBDL+CDL-mediated induction of $Ki67^+$ cells (Figure 4A) and elevation of cyclin E (Figure 4B), which are makers for liver regeneration, in the livers of TNF-$\alpha^{-/-}$ mice was comparable to that in TNF-$\alpha^{+/+}$ mice, suggesting that liver regeneration after CBDL+CDL was not mediated by the

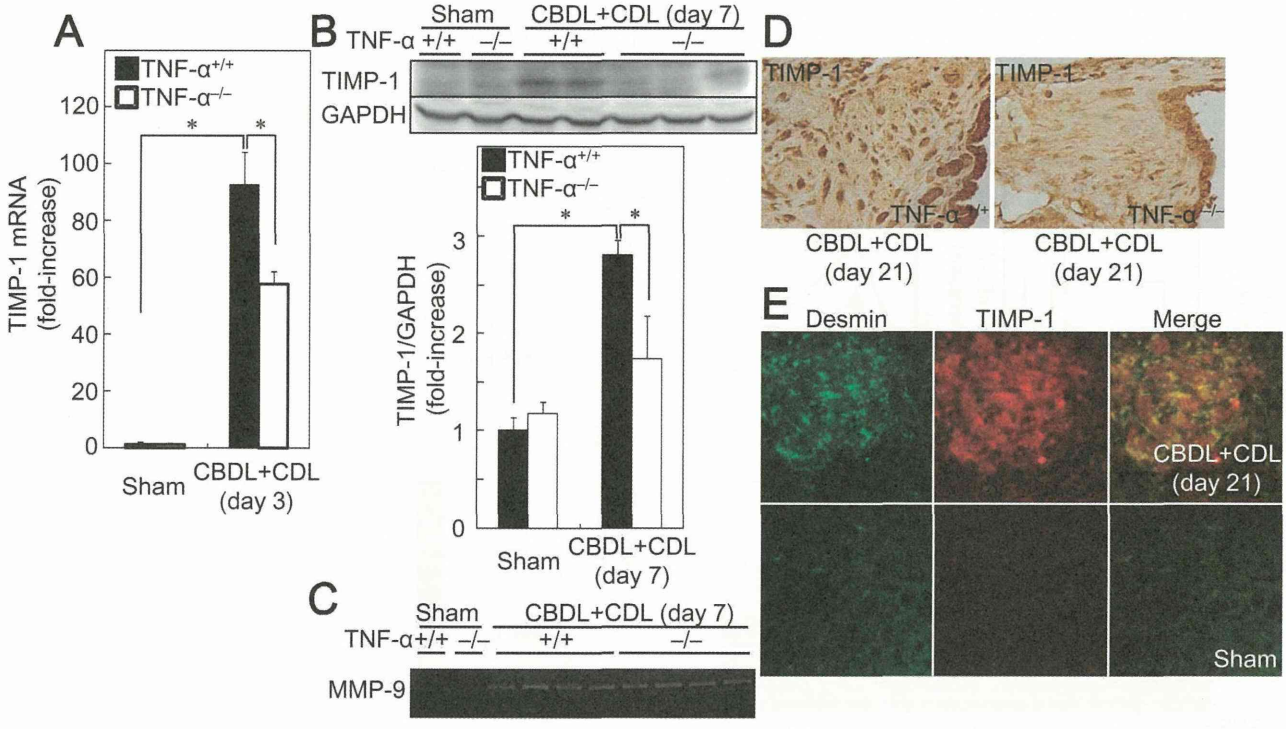

Figure 6. CBDL+CDL increased TIMP-1 in a TNF-α dependent manner. TNF-$\alpha^{+/+}$ and TNF-$\alpha^{-/-}$ mice received CBDL+CDL. The animals were sacrificed at the indicated times. (A) mRNA levels of TIMP-1 in the livers were determined by quantitative real time RT-PCR. (B) The protein extracts from the livers were analyzed by SDS-PAGE, and immunoblotting was performed with anti-TIMP-1 and -GAPDH antibodies. The results shown are representative of at least 5 independent experiments. Relative densitometric intensity of TIMP-1 was determined for each protein band and normalized to GAPDH (bottom panels). (C) Collagenase activities in the protein extracts were measured by gelatin zymography. (D) Expression of TIMP-1 in the livers was examined by immunohistochemistry (original magnification: 400×). (E) Expression of desmin (green) and TIMP-1 (red) around the interstitial space around dilated bile ducts was examined by immunofluorescent staining. The results shown are representative of at least 3 independent experiments. Data are mean ± SD from at least 5 independent experiments. *, P<0.05 using a 2-tailed Student's t-test.
doi:10.1371/journal.pone.0065251.g006

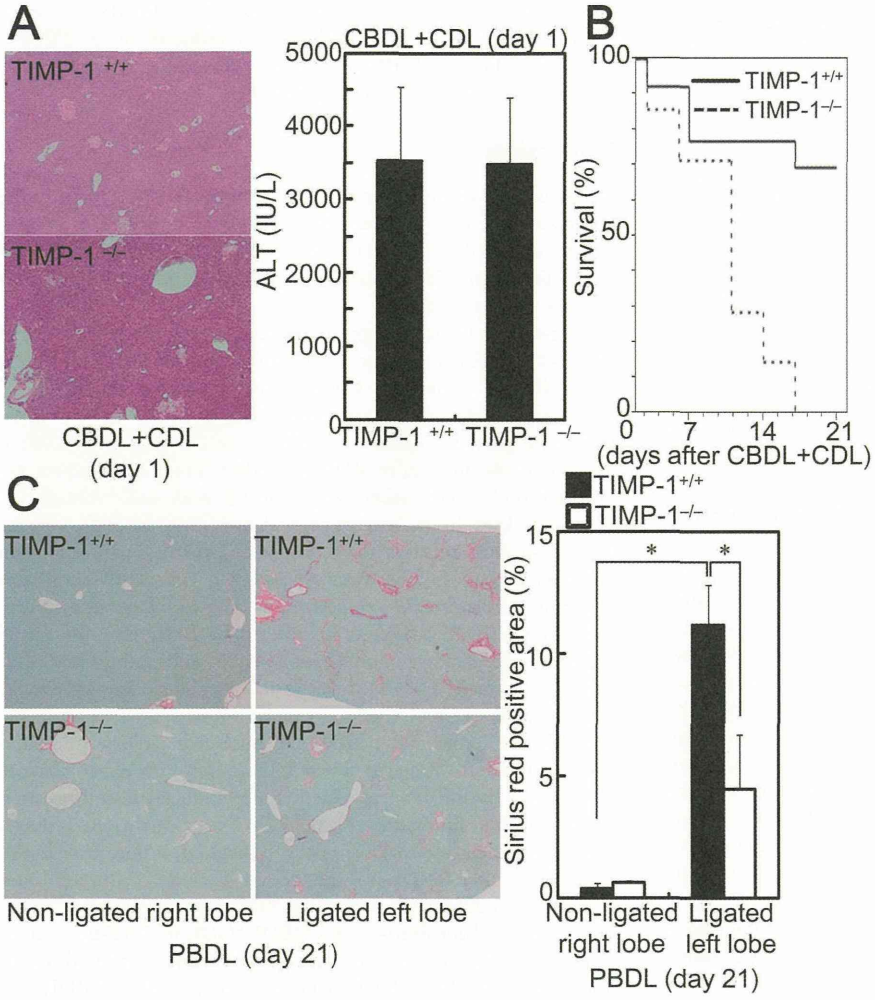

Figure 7. TIMP-1 deficiency reduced liver fibrosis after BDL. TIMP-1$^{+/+}$ and TIMP-1$^{-/-}$ mice received CBDL+CDL (A, B) or PBDL (C). The animals were sacrificed at the indicated times. (A) The injured lesions in the livers were assessed by H&E staining (original magnification: 40×, left panel). Serum ALT levels were compared (right panel). (B) Survival curves for animals with CBDL+CDL. (C) Collagen deposition in the ligated left robes was assessed by Sirius red staining (original magnification: 40×). Sirius red positive area was compared (right panel). Data are mean ± SD from at least 5 independent experiments. *, P<0.05 using a 2-tailed Student's t-test.
doi:10.1371/journal.pone.0065251.g007

produced TNF-α. Thus, the reduced fibrosis in TNF-α$^{-/-}$ mice after CBDL+CDL was not related to the reduction of liver damage or the enhancement of liver regeneration.

TNF-α Decreases Collagen mRNA Expression in Isolated rat HSCs

Because fibrosis was decreased in TNF-α$^{-/-}$ mice, it is possible that TNF-α activates HSCs and increases their collagen production. Indeed, it is reported that TNF-α activates primary cultured HSCs by activation of p38 mitogen-activated protein kinase (MAPK) and c-jun N-terminal kinase (JNK) [32]. To compare the activity status of HSCs between TNF-α$^{+/+}$ and TNF-α$^{-/-}$ mice, we examined expression levels of collagen α1(I) mRNA, TGF-β mRNA, which is an activator of HSCs, desmin and vimentin mRNA, which are classical features of HSCs, and αSMA mRNA and protein, which is a maker for stellate cell activation. The increased CBDL+CDL-mediated expression levels of collagen α1(I) mRNA (Figure 5A), TGF-β mRNA (Figure 5B), αSMA mRNA, desmin mRNA, vimentin mRNA (Table 1), and αSMA protein (Figure 5C) in the livers of TNF-α$^{-/-}$ mice were comparable to those of TNF-α$^{+/+}$ mice, suggesting that TNF-α does not contribute to activation of HSCs and production of collagen in CBDL+CDL mice. To examine the direct effects of TNF-α on collagen expression in HSCs, primary HSCs were isolated from rats and were cultured on plastic dishes, on which the cells were automatically activated and proliferated (Figure 5D). According to the autoactivation, expression levels of collagen α1(I), αSMA, and desmin mRNA in HSCs were increased by culture on plastic dishes for 72 h (Table 2). Exogenous administration of TNF-α decreased the induction of collagen α1(I) mRNA as previously reported [15,16,17], although αSMA was not reduced by TNF-α. Moreover, TNF-α increased desmin and CCL5 mRNA in HSCs (Table 2) which is a mediator of HSC proliferation [33]. Thus, TNF-α decreases collagen α1(I) production without inhibition of activation and proliferation in primary cultured HSCs. These results further suggest that the reduced fibrosis in TNF-α$^{-/-}$ mice is not due to reduction of collagen synthesis in HSCs.